

ONLINE SUPPLEMENTAL MATERIAL

Legends to Supplemental Figures

FIG. S1. **Insulin and IGF-II at equimolar concentration differ in their ability to promote IR-A internalization.** The level of IR-A internalization in R-/IR-A cells was determined by ELISA at different time points after insulin (INS) and IGF-II stimulation, as described in Experimental Procedures. Ligands were used at 30 nM. Data are the averages \pm SD of three independent experiments. Statistical significance was determined using Student's t test for repeated measures, $*p < 0.05$; $***p < 0.01$ (INS or IGF-II vs SFM) and using ANOVA with Bonferroni's multiple-comparison test, $p < 0.01$; (INS vs IGF-II).

FIG. S2. **An insulin analog with lower affinity than insulin for the IR-A induces lower levels of IR-A phosphorylation and signaling.** The insulin analog NMeTyr^{B26}-insulin has been previously described (22). (A) Inhibition of binding of human ¹²⁵I-insulin to the insulin receptor (IR-A isoform) in the membranes of IM-9 lymphocytes by human insulin (●), NMeTyr^{B26}-insulin analog (▲) and human IGF-II (■). Binding was performed as described by Gauguin et al. (23). ^aK_d represents dissociation constant of binding of insulin and insulin analog to the IR. Each value represents the mean \pm the SD of the mean of multiple determinations (n). ^bRelative binding affinity (Rel K_d) defined as (K_d of human insulin/K_d of analog) \times 100. (B) Serum-starved R-/IR-A cells were stimulated with either insulin, IGF-II or NMeTyr^{B26}-insulin at 1, 5 and 30 nM for the indicated time points. IR-A tyrosine-phosphorylation was determined by immunoblot as described in Experimental Procedures. The experiment shown is representative of two independent experiments. (C) Akt and ERK1/2 activation was assessed by immunoblot with anti-phosphospecific antibodies at different time points of ligand stimulation as described above. Blots are representative of two independent experiments.

FIG. S3. **Effect of physiological concentration of ligands on IR-A and IRS-1 stability.** IR-A and IRS-1 levels in R-/IR-A cells were determined by immunoblot after stimulation with 5 nM of either insulin, IGF-II or NMeTyr^{B26}-insulin. The total amount of protein loaded on the gel was monitored using anti- β -actin polyclonal antibodies. Quantification was performed by densitometry using NIH ImageJ software. The data are presented as means \pm SD. Statistical significance was determined using two-way ANOVA with Bonferroni's multiple-comparison test. $***p < 0.001$; $**p < 0.01$; $*p < 0.05$.

FIG. S4. **Insulin and IGF-II differentially affect IR-A internalization of NIH3T3/IR-A, R+A10 and MDA-MB-157 breast cancer cells.** (A, B, C) Protein levels for the IR-A and IGF-IR were determined by immunoblot analysis with specific polyclonal antibodies, as described in Experimental Procedures. (A, B, C) The level of cell surface IR-A in the various cell lines was determined by ELISA at different time points of insulin (INS) and IGF-II stimulation, as described in Experimental Procedures. Data are the averages \pm SD of three independent experiments. Statistical significance was determined using Student's t test for repeated measures, $*p < 0.05$ (INS vs IGF-II). (A, B) IR and IRS-1 levels were assessed as described in Experimental Procedures. Blots are representative of three independent experiments.

Figure S1, Morcavallo et al.

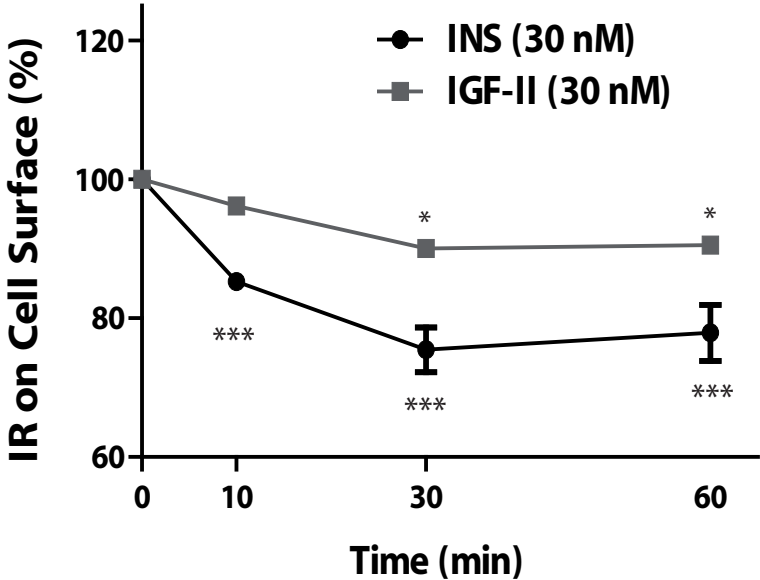


Figure S2, Morcavallo et al.

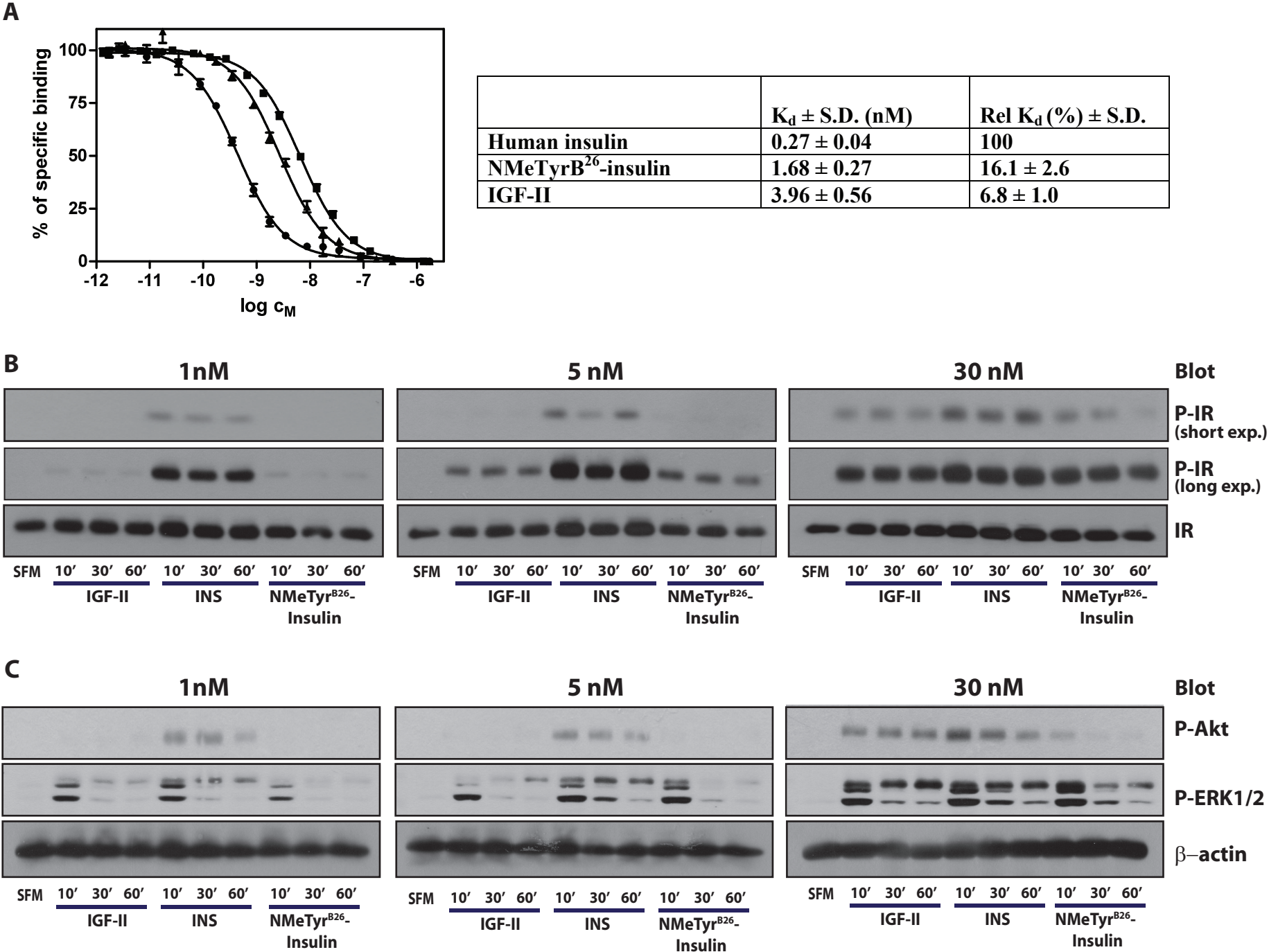


Figure S3, Morcavallo et al.

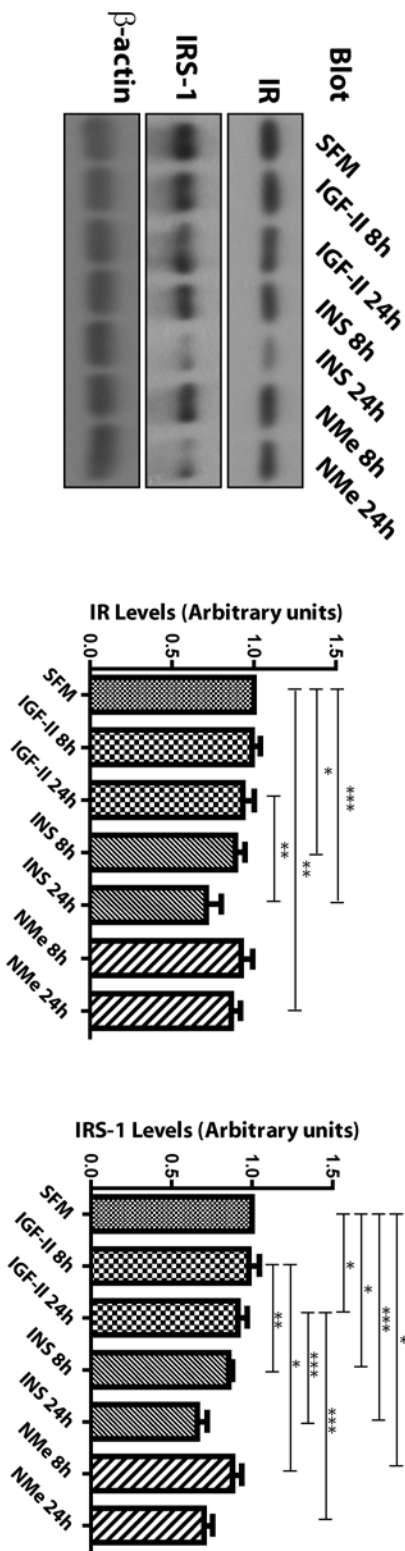


Figure S4, Morcavallo et al.

